

# Nucleation Kinetics of Emulsified Triglyceride Mixtures

William Kloek<sup>1</sup>, Pieter Walstra, and Ton van Vliet<sup>2,\*</sup>

Wageningen University, 6700 EV Wageningen, The Netherlands

**ABSTRACT:** The purpose of this study is to determine characteristic nucleation parameters such as the surface free energy for nucleus formation in mixtures of fully hydrogenated palm oil (HP) in sunflower oil (SF). These parameters will be used to model the bulk crystallization kinetics of the same mixtures. This was achieved by determining the crystallization kinetics in emulsified triglyceride mixtures using differential scanning calorimetry, proton nuclear magnetic resonance, and ultrasound velocity measurements. The latter technique appeared to be very sensitive for monitoring the crystallization kinetics of fat dispersions containing triglycerides with a simple phase behavior. Isothermal crystallization of emulsified HP stabilized by sodium caseinate started at 7 K below the  $\alpha$  clear point, and the kinetics were best fitted assuming heterogeneous nucleation. Isothermal crystallization of emulsified 10% HP in SF stabilized by caseinate started at 14 K below the  $\alpha$  melting point, and the kinetics were best fitted assuming homogeneous nucleation. If the same dispersion was stabilized by Tween 20, crystallization started at 11 K below the  $\alpha$  melting point, and the kinetics were fitted best using heterogeneous nucleation. Analysis of the temperature dependency of the fit parameters yielded a surface free energy of a nucleus of about  $4 \text{ mJ}\cdot\text{m}^{-2}$  in the case of homogeneous nucleation. Pre-exponential nucleation frequencies indicated that a large proportion of the triglyceride molecule should be in the right conformation to be incorporated in a nucleus.

Paper no. J9223 in *JAOCs* 77, 643–652 (June 2000).

**KEY WORDS:** Crystallization, heterogeneous nucleation, homogeneous nucleation, kinetics, nucleation, triglyceride, ultrasound velocity.

Nucleation is an essential step in crystallization, but it also is the step that is least accessible to experiments. Nucleation is the formation of ordered domains by random association of molecules up to a certain critical size. It determines how many crystals will be formed and therefore their final average size. A dispersion of fat crystals with a large number of small crystals may have desired properties such as a good spreadability but for crystal separation purposes it is undesired.

<sup>1</sup>Present affiliation: DMV-International, P.O. Box 13, 5460 BA Veghel, The Netherlands.

<sup>2</sup>Wageningen Centre for Food Sciences, P.O. Box 8129, 6700 AN, Wageningen, The Netherlands.

\*To whom correspondence should be addressed at: Wageningen Agricultural University, Department of Food and Nutritional Science, Food Physics Group, P.O. Box 8129, 6700 EV Wageningen, The Netherlands.  
E-mail: Ton.vanVliet@phys.fdsci.wau.nl

With homogeneous nucleation, no surface acts as catalyst: the crystallizing molecules spontaneously form nuclei. Homogeneous nucleation conditions are normally reached only when the solution or melt is dispersed into a number of droplets that exceeds the number of catalytic impurities present in the system. For crystallization of dispersed tristearate and tripalmitate, supercooling of up to 26 K in the  $\alpha$  polymorph was observed (1,2). For emulsified milk fat, supercooling up to 20 K below the  $\alpha$  clear point was obtained (3).

In bulk fats, supercooling of only a few K is needed to induce crystallization. This is explained by the presence of (solid) impurities of a size larger than the dimensions of a nucleus. These impurities can act as a catalyst for nucleation by lowering the activation Gibbs energy for formation of a nucleus. It is assumed that nucleation in bulk fats will often be heterogeneous (4).

The concentration of catalytic impurities is important for modeling the crystallization kinetics of bulk fats. To determine the effect of impurities on crystallization kinetics, the crystallizing phase has to be divided in such volumes that at most one catalytic impurity per droplet is present. This can be achieved by emulsifying the fat phase. If the fat is divided over a number of droplets that is very large compared to the number of catalytic impurities per volume, homogeneous nucleation will predominate. The appendix to this paper gives a short description of the model and the associated equations for homogeneous and heterogeneous nucleation in emulsions. The classic equations for the nucleation rate  $J$ , which is the number of nuclei that are formed per unit volume and unit time, are also given in the Appendix.

The purpose of the study presented in this paper was to determine characteristic nucleation parameters such as the surface free energy for nucleus formation and the number of catalytic impurities in mixtures of fully hydrogenated palm oil (HP) in sunflower oil (SF). This is done by determining the crystallization behavior of emulsified fats. The obtained parameters will be used to model the bulk crystallization kinetics of the same mixtures (7).

## EXPERIMENTAL PROCEDURES

**Materials.** The model system consists of mixtures of HP and SF, HP being the solid phase and SF being the liquid phase. None of the fats was purified. The fatty acid composition of the HP and SF is given in Table 1.

**TABLE 1**  
Fatty Acid Composition (w/w) of Sunflower Oil (SF)  
and Fully Hydrogenated Palm Oil (HP)<sup>a</sup>

Fatty acid	Code	Percentage in HP	Percentage in SF
C12:0	L	0.3	
C14:0	M	1.0	0.1
C16:0	P	41.3	6.1
C18:0	S	55.9	2.2
C18:1	O	0.1	27.3
C18:2	I		64.2
C20:0	A	1.0	
C22:0	B	0.3	

<sup>a</sup>Fatty acid codes Cx:y; x = number of C-atoms; y = number of unsaturated bonds.

HP contains less than 1% monoglycerides, about 6% diglycerides, and about 94% triglycerides. The triglycerides in HP mainly contain stearic acid and palmitic acid. The triglyceride composition is calculated from the total fatty acid composition and the composition of the fatty acids esterified at the 2-position of glycerol, assuming random distribution of the fatty acids over the positions 1 and 3.

Only the combinations containing stearic acid and palmitic acid were considered. Table 2 shows that the HP would be rich in the triglycerides PSS, PSP, and SSS (where P = palmitic acid and S = stearic acid). Besides the triglyceride composition, the melting temperatures  $T_{m,i}$  and the enthalpies of fusion  $\Delta H_{f,i}$  of the various polymorphs also have been compiled (5). The  $T_m$  values for the triglycerides are all far above room temperature, so at these conditions HP is a hard fat. SF started to crystallize at a temperature of about  $-5^\circ\text{C}$ . Since experiments were only carried out at temperatures above  $0^\circ\text{C}$ , no data about the triglyceride composition of SF and its thermal behavior are given.

Thermodynamic parameters of the model system were determined by measuring the crystallization temperature  $T$  of the  $\alpha$  polymorph (rapid cooling) and the melting temperature  $T$  of the  $\beta'$  polymorph (after isothermal crystallization above the  $\alpha$  melting temperature) as a function of the mole fraction HP,  $x_{\text{HP}}$ , by differential scanning calorimetry (DSC). The temperatures  $T$  were the peak temperatures in the thermo-

grams. From the temperatures obtained at various mole fractions of HP,  $\Delta H_{f,i}$  and  $T_{m,i}$  of the pure HP in polymorph  $i$  were calculated assuming ideal mixing, using the following equation (5,6):

$$\ln x_{\text{HP}} = \frac{\Delta H_{f,i}}{R_g} \cdot \left( \frac{1}{T} - \frac{1}{T_{m,i}} \right) \quad [1]$$

where  $R_g$  is the gas constant. More detailed analyses on the phase behavior of HP/SF mixtures have been given (7). These results, which could only be obtained for the  $\alpha$  and the  $\beta'$  polymorphs, are as follows. For HP, the calculated average molar mass, based on triglyceride composition, was  $854 \text{ g}\cdot\text{mol}^{-1}$ ;  $T_{m,\alpha}$ ,  $41.8^\circ\text{C}$ ;  $\Delta H_{f,\alpha}$ ,  $9.8\cdot 10^4 \text{ J}\cdot\text{mol}^{-1}$ ;  $T_{m,\beta'}$ ,  $57.3^\circ\text{C}$ ;  $\Delta H_{f,\beta'}$ ,  $1.61\cdot 10^5 \text{ J}\cdot\text{mol}^{-1}$ ; for SF, the molar mass was  $877 \text{ g}\cdot\text{mol}^{-1}$ .

**Emulsion preparation.** The aqueous phase of the emulsions consisted of 2% (w/w) freeze-dried sodium caseinate in 0.005 M sodium chloride (pH = 6.9), or 1% Tween 20. Sodium caseinate was chosen as an emulsifier because it provides superior protection against partial coalescence of the partially crystallized droplets. If appropriate, SF was added to the aqueous phase at room temperature. Subsequently, HP was melted at  $80^\circ\text{C}$  and then added to the unheated aqueous phase. Every emulsion contained 20% (w/w) dispersed phase. The percentage of HP in the dispersed phase was varied.

Prior to pre-emulsification, the mixture was heated to  $75^\circ\text{C}$  to ensure that all HP had melted. A pre-emulsion was made by mixing in a Waring Blendor (TE, Schagen, The Netherlands) or an Ultra-Turrax (Brussels, Belgium) for 15 s. This pre-emulsion was homogenized with a high-pressure homogenizer (Foss Electric, Hillerod, Denmark; Shields, or Rannie, Crawly, United Kingdom). To avoid crystallization of HP in the homogenizer, it was first rinsed with water of  $75^\circ\text{C}$  for 15 min. Before using an emulsion, it was heated to  $75^\circ\text{C}$  for 15 min to melt the HP and to destroy any crystal memory.

The particle size distribution of the emulsions was determined using a Coulter Counter Multisizer (Fullerton, CA) or a Malvern Master Sizer (Worcester, United Kingdom). From this distribution some characteristic droplet size ( $d_{ab}$ ) (where a and b are Euclidian dimensions) and the relative standard deviation of the droplet size distribution ( $C_x$ ) were calculated

**TABLE 2**  
Triglyceride Composition of HP Calculated from the Total Fatty Acid Composition  
and the Composition of the Fatty Acids Esterified at the 2-Position of Glycerol<sup>a</sup>

Triglyceride	(%)	$T_{m,\alpha}$ ( $^\circ\text{C}$ )	$\Delta H_{f,\alpha}$ ( $\text{kJ}\cdot\text{mol}^{-1}$ )	$T_{m,\beta'}$ ( $^\circ\text{C}$ )	$\Delta H_{f,\beta'}$ ( $\text{kJ}\cdot\text{mol}^{-1}$ )	$T_{m,\beta}$ ( $^\circ\text{C}$ )	$\Delta H_{f,\beta}$ ( $\text{kJ}\cdot\text{mol}^{-1}$ )
PPP	4.0	44.7	95.8	55.7	126.5	65.9	171.3
PSP	26.1	47.2	112.2	67.7	165.5	65.3	173.6
PSS	39.0	50.1	106.0	61.8	—	64.4	172.9
SSS	14.5	54.7	108.5	64.3	156.5	72.5	194.2
PPS	6.0	46.4	100.0	58.7	124.0	62.6	166.3
SPS	2.2	50.7	103.0	—	—	68.0	170.3

<sup>a</sup>Assuming random distribution of the fatty acids over the 1- and 3-positions. Only triglycerides containing palmitic acid (P) and stearic acid (S) are taken into account. Also, melting temperatures ( $T_m$ ) and enthalpies of fusion ( $\Delta H_{f,i}$ ) of the pure triglycerides in polymorph  $i$  are compiled from Reference 5.

using the following equations, in which  $n_i$  is the number of droplets in a size class of mean diameter  $d_i$ .

$$d_{ab} = \left( \frac{S_a}{S_b} \right)^{1/(a-b)} \quad \text{with } S_x = \sum_i n_i \cdot d_i^x$$

$$C_x = \sqrt{\frac{S_x \cdot S_{x+2}}{S_{x+1}^2} - 1} \quad [2]$$

The characteristics are compiled in Table 3.

**Proton nuclear magnetic resonance (p-NMR).** The p-NMR used was a Bruker-minispec P20i (Karlsruhe, Germany). NMR tubes were filled with a known weight of emulsion (about 0.8 g.). For determination of the amount of solid fat, only the liquid signals were measured. The solid fat content of a crystallizing emulsion could be determined by measuring the liquid signal of the emulsion ( $S_{em}$ ), the liquid signal of a completely solidified emulsion ( $S_{sol}$ ), and the liquid signal of a nonsolidified emulsion ( $S_{liq}$ ) (8,9):

$$\phi = \frac{S_{em} - S_{liq}}{S_{sol} - S_{liq}} \quad [3]$$

Prior to isothermal crystallization experiments, a cooling–heating scan was performed to determine the temperature at which crystallization started.

**DSC.** Experiments were carried out using a PerkinElmer DSC-7 (Norwalk, CT). Emulsions were crystallized by cooling the emulsion from 80 to 5°C at a rate of 2 K·min<sup>-1</sup>. After keeping the sample for 2 min at 5°C, it was then heated at a rate of 2 K·min<sup>-1</sup> to determine the melting endotherm.

**Ultrasound velocity.** In a mixture of  $i$  components (phases), the ultrasound velocity is a function of the volume average of the density and the adiabatic compressibility; it increases with a decrease of density or compressibility or both (10). It is not necessary to determine these parameters at the experimental conditions to calculate the volume fractions since they can be calculated from the velocities of the individual components. In the case of emulsified fats, the volume fraction of solidified droplets can be calculated if the ultrasound velocity in an emulsion with completely liquid droplets

( $v_l$ ) and completely solid droplets ( $v_s$ ) is known at a comparable temperature. The volume fraction of solids  $\phi$  can be calculated by the Urick equation (10,11):

$$\phi = \left[ \frac{(1/v^2) - (1/v_l^2)}{(1/v_s^2) - (1/v_l^2)} \right] \cdot \phi_d \quad [4]$$

where  $\phi_d$  is the volume fraction of the crystallizing component in the dispersed phase. An advantage of using the solid and liquid velocities of the dispersed system is that no correction has to be made for scattering by the dispersed particles.

The ultrasound cell was filled with 75 mL emulsion and placed in a waterbath for temperature control. The time for the sound pulse to travel twice the diameter of the cell was measured by the ultrasonic velocity meter (UVM1; Cygnus Instruments, Darchester, United Kingdom). Temperature, velocity, and time were on-line transmitted to a spreadsheet. Every minute, average readings of the velocity and of the temperature were made. The timing accuracy was 0.01  $\mu$ s in the range of 10–200  $\mu$ s. The velocity could be measured with an accuracy of 0.1 m·s<sup>-1</sup>. The temperature precision was 0.01 K and the temperature accuracy inside the cell was 0.05 K. Prior to isothermal crystallization experiments, a cooling–heating scan was made to determine at what temperature the emulsion started to crystallize. This temperature scan was also used to determine the dependency of the solid and liquid velocities of the emulsions on temperature.

## RESULTS

**p-NMR and DSC.** p-NMR and DSC experiments could only be used to determine the onset temperature for crystallization of the emulsions. These are, together with the parameters characterizing the droplet size distribution, compiled in Table 4 and will be discussed later. It was not possible to do accurate isothermal crystallization experiments using both methods. The differential nature of DSC caused heat fluxes that were too small to allow accurate determinations. Moreover, the time needed for stabilization of the baseline after bringing the sample to the isothermal temperature was too long. For the p-NMR experiments the change in liquid signal was too small to allow accurate determination of the fraction of crystallized droplets.

**Ultrasound velocity. (i) Cooling–heating cycles.** Cooling–heating cycles of SF, water, and SF in water emulsions were similar to those discussed by Dickinson *et al.* (12) and are therefore not shown. Figure 1 shows the effects of cooling (from 80 to 20°C) and heating (from 20 to 80°C) of an HP emulsion on ultrasound velocity. The curves are similar to those of a palm oil-in-water emulsion measured by Hodate *et al.* (13). On cooling, the velocity initially followed a third-degree polynomial, as in the case of the SF emulsion. At 35°C the ultrasound velocity clearly started to increase steeply with decreasing temperature from 1480 m·s<sup>-1</sup> to about 1550 m·s<sup>-1</sup> at 30.5°C due to crystallization of the HP. Crystallization of the HP would result in an increase in density and a decrease

**TABLE 3**  
Characteristic Parameters Calculated from the Droplet Size Distribution of Emulsified HP/SF Mixtures with a Fat Content of 20% (w/w)<sup>a</sup>

HP/SF (%)	Continuous phase	Homogenizer; number of passes	$d_{32}$ ( $\mu$ m)	$C_2$ ( $\mu$ m)
100	Caseinate	Shields; 1	0.54	0.68
100	Caseinate	Foss; 8	1.13	—
25	Caseinate	Rannie 5 bar; 6	2.93	0.40
25	Caseinate	Rannie 10 bar; 6	1.96	0.44
25	Caseinate	Rannie 20 bar; 6	1.13	0.45
10	Caseinate	Shields; 2	0.41	0.56
10	Caseinate	Shields; 6	0.39	0.51
10	Tween 20	Shields; 6	0.38	0.50
0	Caseinate	Shields; 2	0.47	0.53

<sup>a</sup> $d_{ab}$ , characteristic droplet size;  $C_x$ , relative standard deviation of the droplet size distribution. For abbreviations see Table 1.

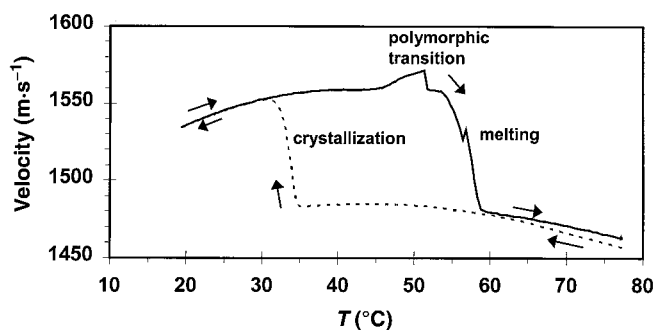


FIG. 1. Ultrasound velocity of a hydrogenated palm oil emulsion ( $\phi = 0.20$ ) as a function of temperature on subsequent cooling (dotted line) and heating (solid line).

in compressibility. The increase of the ultrasound velocity due to crystallization shows that the relative change in compressibility is greater than the relative change in density. On further cooling after crystallization, the velocity decreased with decreasing temperature. On heating after cooling, the velocity initially followed the cooling line, indicating that the emulsion was not destabilized at this stage. At temperatures above the crystallization temperature, the velocity also followed a cubic curve like the SF in water emulsion indicating that no melting process occurred. Around 48°C the velocity increased over a temperature interval of about 7°C. At 52°C the velocity suddenly dropped as the melting process started. The increase of the velocity could have been caused by a polymorphic transition from  $\alpha$  to a mixture of mainly  $\beta$  and some  $\beta'$ , because a more stable polymorph will have a lower compressibility. Between 55 and 59°C the velocity decreased strongly, owing to melting of the crystals. This melting temperature agrees well with the melting temperatures of the  $\beta'$  polymorph or the  $\beta$  polymorph of HP. After the HP had completely melted ( $T > 59^\circ\text{C}$ ), the heating curve initially followed the cooling curve but soon deviated from the cooling curve. This deviation was most likely caused by some coalescence of the emulsion droplets, resulting in creaming of oil droplets; the emulsion was not homogeneous anymore, and the measured velocity no longer corresponded with the initial emulsion. Since destabilization of the emulsion only occurred after melting of the crystallized emulsion during stirring and not during cooling, it is unlikely that destabilization would occur during isothermal crystallization.

The increase of the sound velocity on crystallization of a 20% emulsion was approximately  $70 \text{ m}\cdot\text{s}^{-1}$ . The accuracy of the velocity measurement is  $0.1 \text{ m}\cdot\text{s}^{-1}$ ; this means that the amount of solid fat can be determined with an accuracy of 0.3%. This is much better than the accuracy of 1.5% that was reached by the p-NMR method.

Figure 2 shows a cooling–heating cycle of a 20% emulsion where the dispersed phase consisted of 10% HP/SF. The general form of the curve is comparable to that of the 100% HP emulsion. Crystallization of emulsified 10% HP/SF occurred at a much lower temperature than of emulsified HP/SF. Instead of showing an increase in velocity on crystallization,

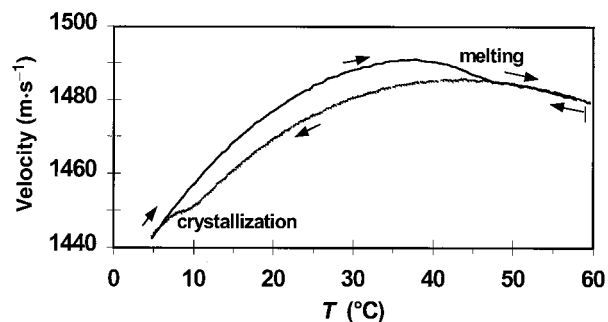


FIG. 2. Ultrasound velocity of emulsified 10% hydrogenated palm oil/sunflower oil (HP/SF) using sodium caseinate as emulsifier as a function of temperature on subsequent cooling from 60 to 5°C and heating back to 60°C.

only a smaller decrease in velocity on cooling was seen. This can be explained by the higher negative value of the temperature coefficient of the velocity due to the presence of SF.

The heating curve initially followed the cooling curve, indicating that virtually all HP had crystallized over a narrow temperature range and that no appreciable demixing or polymorphic transition had occurred. The melting process started around 35°C. After melting was complete, the velocity was the same as for the cooling curve. This shows that no significant coalescence had occurred. After the first cooling–heating cycle, a second one was performed. This curve perfectly matched the first cooling–heating curve. The heating curve showed no indication for a polymorphic transition from  $\alpha$  to  $\beta$  or  $\beta'$ . The time scales of this transition in 10% HP/SF dispersions were 30 and 3 min at temperatures of 5 and 15°C, respectively (7). In taking these time scales into account, the polymorphic transition was expected to occur at a temperature of about 14°C. The increase in velocity due to a polymorphic transition was possibly too small to be noticed.

The supercooling needed for crystallization of emulsified 10% HP/SF was 13°C for the  $\alpha$  polymorph and 34°C for the  $\beta'$  polymorph. These supercoolings were higher than the supercooling for emulsified 100% HP which were 7 and 22°C for the  $\alpha$  and  $\beta'$  polymorph, respectively. If nucleation is heterogeneous, this would indicate that the HP contained most of the impurities.

Emulsified 10% HP/SF with Tween 20 as the emulsifier gave a velocity–temperature curve of the same shape. Crystallization started at 13°C, which is 3°C higher than for sodium caseinate as the emulsifier. The hydrophobic lauryl chain of Tween 20 possibly induces structuring of the triglyceride molecules near the droplet boundary so that a smaller Gibbs activation energy would be needed for nucleation, and therefore the crystallization temperature will be higher. The increase in crystallization temperature as result of a more hydrophobic emulsifier was also observed by Kaneko *et al.* (14). The melting process started at the same temperature as for the sodium caseinate-stabilized 10% HP/SF emulsion. The emulsion also appeared to be stable against (partial) coalescence, despite a less protective emulsifier. Repeated temperature cycles with

the same emulsion gave velocity–temperature curves that perfectly matched the curve obtained in the first cycle.

**Isothermal crystallization.** Isothermal crystallization experiments were carried out on HP emulsions at temperatures that were selected on the basis of cooling–heating cycles. The sound velocities in dispersions containing completely solid or completely liquid droplets as a function of temperature were described by curvilinear regression. The volume fraction of solidified droplets was calculated by the Urick equation. After introduction of the emulsion in the ultrasound cell, it took about 4–5 min for the temperature to reach its final value. During this time crystallization should not occur. At high supercoolings, a little crystallization sometimes occurred before the final temperature was reached. This will have some effect on the results at the beginning of the crystallization process but it will not affect the crystallization curve after, say, 10 min. For the calculation of the fraction of solidified droplets from the liquid and solid velocities, the actual temperatures were used.

Figure 3 shows that the (initial) crystallization rate of emulsified HP (sodium caseinate as emulsifier) increased with decreasing temperature. After 90 min the crystallization rate decreased to very low values. The fraction of solidified droplets increased with decreasing crystallization temperature. This can be explained by heterogeneous nucleation: at lower temperatures the fraction of droplets void of catalytic impurities was smaller so the fraction of droplets that had not crystallized would also be smaller. If nucleation would be

homogeneous, crystallization would proceed until all droplets had crystallized.

The crystallization curves were fitted to homogeneous and heterogeneous nucleation models taking into account the droplet size distribution (Fig. 3). The experimental crystallization curves were fitted best by a heterogeneous nucleation model, although it should be remembered that the heterogeneous model contains two fit parameters (the maximum nucleation rate  $J_0$  and the number density of impurities  $N_{imp}$ ), whereas the homogeneous nucleation model has only one fit parameter (the nucleation rate). The initial crystallization rate is somewhat overestimated which can be explained by the temperature not having reached its final value in the first few minutes and possibly by production of crystallization heat.

According to Equations A-1 and A-2 in the Appendix, it is possible to extract the Gibbs surface energy  $\gamma$  for (heterogeneous) nucleation from the slope of a plot of  $\ln J_0$  against a supercooling term. Figure 4A shows a linear relation between  $\ln J_0$  and the supercooling term. The obtained slope corresponds to a value for the Gibbs surface energy for a nucleus of  $2.6 \text{ mJ}\cdot\text{m}^{-2}$ . However, as the type of nucleation is heterogeneous, the liquid–solid contact angle is smaller than  $180^\circ$  and therefore the surface Gibbs energy for nucleation would be higher than  $2.6 \text{ mJ}\cdot\text{m}^{-2}$ .

According to Walstra and van Beresteyn (3), the number density of catalytic impurities increases with decreasing temperature, often following the empirical relation  $\log N_{imp} = A - B\cdot T$ . Figure 4B shows a negative correlation between the number of impurities and temperature. Coefficient  $B$  expresses the temperature sensitivity of the number density of

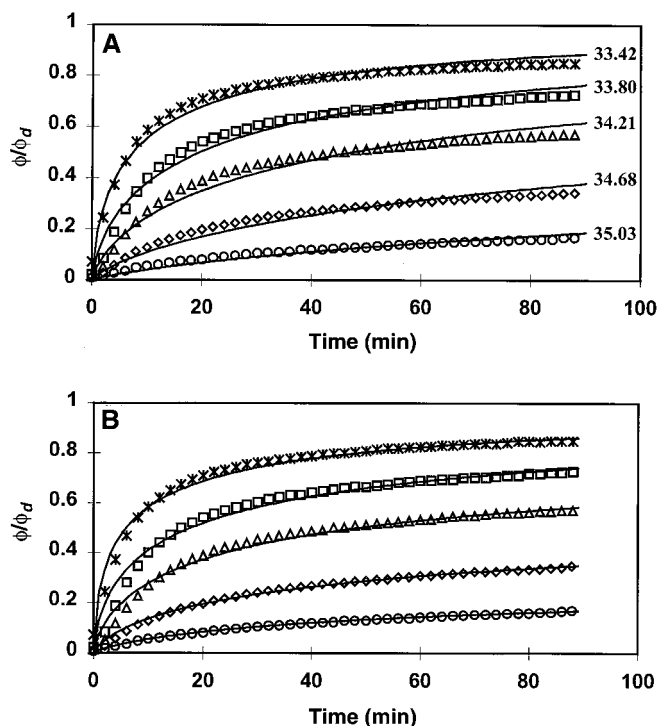


FIG. 3. Measured (symbols) and fitted isothermal crystallization curves (solid lines) of emulsified HP using (A) a homogeneous volume nucleation model and (B) a heterogeneous nucleation model. Crystallization temperatures are indicated in °C. For abbreviation see Figure 2.

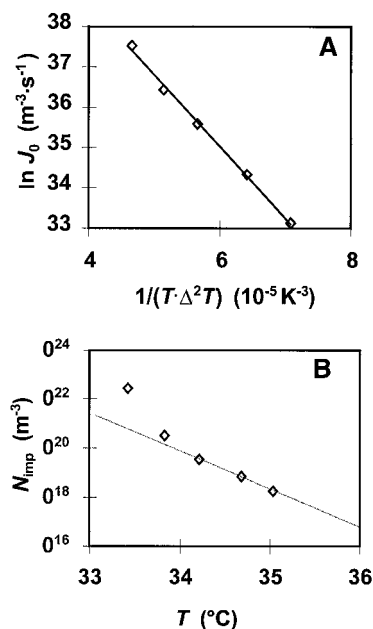


FIG. 4. Fitted maximum nucleation rate  $J_0$  as function of a supercooling term (A), and the number density of catalytic impurities  $N_{imp}$  vs. temperature (B), both obtained from crystallization kinetics of emulsified HP using sodium caseinate as the emulsifier. Nucleation is assumed to occur in the  $\alpha$  polymorph. For abbreviation see Figure 2.

catalytic impurities and is about  $1 \text{ K}^{-1}$  in the temperature range of  $34\text{--}35^\circ\text{C}$ : this means an increase of  $N_{\text{imp}}$  by a factor 10 for a decrease in temperature by 1 K. This value is very high. Walstra and van Beresteyn determined  $B$  to be  $0.17 \text{ K}^{-1}$  for emulsified milk fat, which means an increase of  $N_{\text{imp}}$  by a factor of 1.5 over 1 K. At lower temperatures the logarithm of  $N_{\text{imp}}$  increases more than linearly with decreasing temperature. This can be due to the high values of  $N_{\text{imp}}$ , so that the term  $1 - \exp(-v_d \cdot N_{\text{imp}})$  (Eq. A-4) becomes insensitive to  $N_{\text{imp}}$ .

In order to determine at which conditions homogeneous nucleation occurs, it is necessary to decrease the number of impurities per droplet. This can be achieved by dispersing the fat phase into smaller droplets or by diluting the HP with SF. Since it was not possible to homogenize at various pressures during these experiments, the HP was diluted 10 times with SF. An additional advantage is that the composition of the fat phase is close to that of the dispersions used for the rheological and bulk crystallization studies. A disadvantage is that a whole new range of triglycerides containing unsaturated fatty acids is introduced and that the temperature at which crystallization starts will be much lower.

Figure 5 shows the isothermal crystallization curves of emulsified 10% HP/SF stabilized with sodium caseinate. They are described well by assuming nucleation to be homogeneous. It was not possible to distinguish between volume or surface nucleation. Fitting the crystallization curves by a heterogeneous model showed significantly poorer fits for all temperatures. A plot of  $\ln J$  against a supercooling term again yields a straight line (Fig. 6). The slope corresponds to a Gibbs surface energy for a nucleus of  $4.1 \text{ mJ}\cdot\text{m}^{-2}$ , and the intercept yields a pre-exponential term of  $1.9 \cdot 10^{21} \text{ m}^{-3}\cdot\text{s}^{-1}$ . The Gibbs surface energy is significantly higher than the value obtained from the maximal heterogeneous nucleation rates for emulsified HP.

On diluting the solid phase 10 times with SF, the nucleation type apparently changes from heterogeneous to homogeneous, if it is assumed that the nucleation of emulsified HP is of a heterogeneous nature. This may be explained by dilution of HP so that the concentration of the catalytic impurities

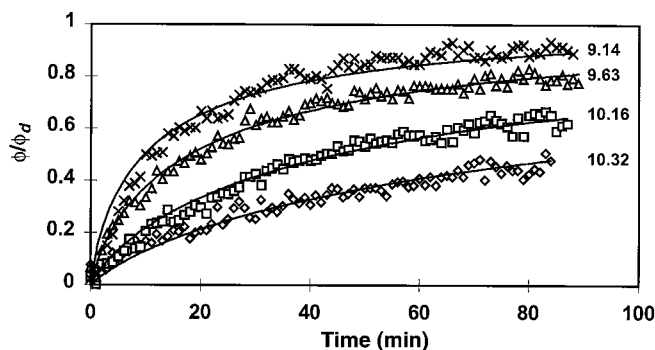


FIG. 5. The volume fraction of droplets containing solid fat during isothermal crystallization of emulsified 10% HP/SF using sodium caseinate as emulsifier at various temperatures (indicated in  $^\circ\text{C}$ ). The solid lines are fits assuming homogeneous nucleation. For abbreviations see Figure 2.

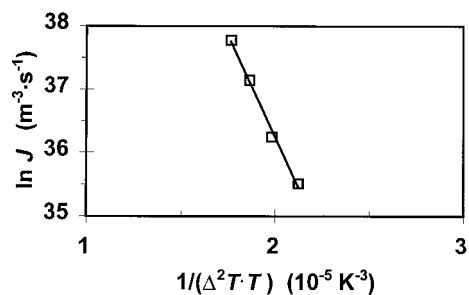


FIG. 6. Fitted nucleation rates assuming homogeneous nucleation of emulsified 10% HP/SF stabilized with sodium caseinate as function of a supercooling term. For abbreviations see Figure 2.

is decreased by a factor 10. The decrease of this number can be even much higher if micelles of monoglycerides are the catalytic impurities, since it is possible that the critical micelle concentration is not reached.

It was shown earlier that the presence of Tween 20, a molecule containing a lauryl chain, increased the onset crystallization temperature of emulsified 10% HP/SF by about 3 K. This effect of a hydrophobic emulsifier was also shown by Kaneko *et al.* (14). This was tentatively explained by structuring of the triglycerides near the droplet boundary, although one should keep in mind that Tween 20 contains a rather bulky hydrophilic group that will hinder a close packing of lauryl chains in the oil phase. If the adsorption layer consist of pure Tween 20, the droplet boundary would be expected to act as a catalytic impurity: hence, nucleation kinetics should then be modeled by a homogeneous model with decreased effective surface energy.

Figure 7 shows that the nucleation kinetics of Tween 20 that stabilized dispersed 10% HP/SF are best described by a heterogeneous nucleation model. The surface fit is slightly better than the volume fit (results not shown). A possible explanation is that not the whole droplet boundary is catalytic, but only some regions at the droplet boundary where particu-

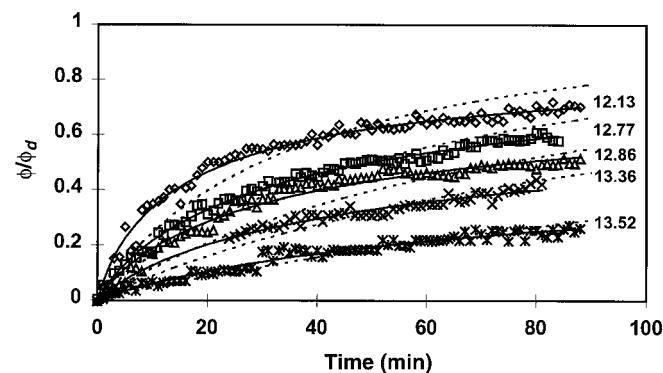


FIG. 7. The volume fraction of droplets containing solid fat during isothermal crystallization of emulsified 10% HP/SF using Tween 20 as the emulsifier at various temperatures (indicated in  $^\circ\text{C}$ ) as a function of time. The solid lines are fits assuming heterogeneous and the dotted lines assuming homogeneous nucleation. For abbreviations see Figure 2.

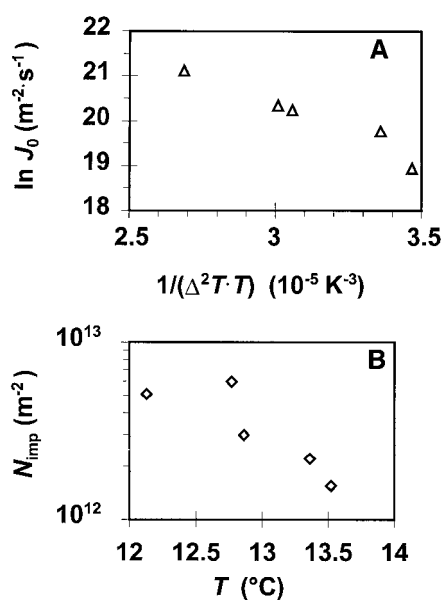


FIG. 8. Fitted maximum surface nucleation rate  $J_0$  (A), and number density of catalytic impurities  $N_{\text{imp}}$  (B), as function of a supercooling term and temperature, respectively, as obtained from crystallization kinetics of emulsified 10% HP/SF using Tween 20 as the emulsifier. The supercooling term is calculated by assuming that nucleation occurred in the  $\alpha$  polymorph. For abbreviations see Figure 2.

lar impurities from Tween 20 would be adsorbed. Figure 8a shows that there is a roughly linear relation between  $\ln J_0$  and the supercooling term. The number of impurities per unit surface area would be about  $10^{12}$  per  $\text{m}^2$ , which decreases slightly with increasing temperature as can be seen from Figure 8B. Assuming an average droplet diameter of  $0.38\ \mu\text{m}$  yields about 0.5 catalytic impurities per droplet for  $N_{\text{imp}} = 10^{12}\ \text{m}^{-2}$ . Figure 8 shows that the fits are poorer compared to the fit of  $\ln J$  vs. the supercooling term of 10% HP/SF dispersions stabilized with sodium caseinate (Fig. 6). The fit parameters obtained at a temperature of  $12.8^{\circ}\text{C}$  (i.e., a supercooling term of  $3.01 \cdot 10^{-5}\ \text{K}^{-3}$ ) especially seem to deviate from the fit parameters obtained at other temperatures.

## DISCUSSION

Table 4 summarizes the supercooling needed to initiate crystallization in emulsified HP/SF mixtures and the type of nucleation that was derived from the crystallization kinetics for the experiments described. The supercooling in the  $\alpha$  polymorph needed to initiate crystallization of emulsified HP is about 7 K. This low supercooling suggests that crystallization is initiated by heterogeneous nucleation, because for homogeneous nucleation of purified fats supercooling up to 26 K is reported. The type of nucleation that was derived from the crystallization kinetics of emulsified HP was also of a heterogeneous nature. However, the supercooling of emulsified HP is independent of the average droplet size, as follows from the crystallization temperatures observed in NMR and ultrasound experiments. This suggests that the nucleation of emulsified

TABLE 4  
Onset Crystallization Temperature  $T_{c\text{-onset}}$  and Supercooling  $\Delta T$  in the  $\alpha$  Polymorph of HP/SF Emulsions with Various Average Particle Sizes, Determined with Different Techniques<sup>a</sup>

HP (%)	Technique	Emulsifier	$d_{32}$ ( $\mu\text{m}$ )	$T_{c\text{-onset}}$ ( $^{\circ}\text{C}$ )	$\Delta T$ (K)	Nucleation type (from kinetics)
100	NMR	Caseinate	1.13	35	7	—
50	NMR	Caseinate	1.12	27	9	—
25	NMR	Caseinate	1.13	19	12	—
25	DSC	Caseinate	1.13	19	12	—
100	Ultrasound	Caseinate	0.54	35	7	Heterogeneous
10	Ultrasound	Caseinate	0.39	10	14	Homogeneous
10	Ultrasound	Tween 20	0.38	13	11	Heterogeneous

<sup>a</sup>The type of nucleation is derived from the crystallization kinetics. NMR, nuclear magnetic resonance; DSC, differential scanning calorimetry; for other abbreviations see Tables 1 and 4.

HP is not catalyzed by impurities and thus is homogeneous because the reduction of the number of impurities per droplet by a factor  $(1.13/0.54)^3 = 9.2$  did not lead to a lower onset crystallization temperature.

If the HP is diluted with SF, the maximum supercooling increases from 7 K for 100% HP to 14 K for 10% HP/SF. A more relevant term to indicate the supercooling is the supersaturation, because this is the driving force for crystallization. The supersaturation is given by  $\ln \beta$  where  $\beta$  is the ratio between the mole fraction HP present and the mole fraction soluble HP as expressed by the Hildebrand equation (Eq. 1). The supersaturation needed to initiate crystallization can be calculated from Equation A-2 and yields values ranging from 0.83 for 100% HP to 1.90 for 10% HP/SF. The crystallization kinetics of emulsified 10% HP/SF could be described by only one nucleation rate for all droplet sizes and therefore nucleation seems to be homogeneous. On the other hand, the supercooling needed relative to the bulk melting temperature of the  $\alpha$  polymorph is only 14 K and suggests heterogeneous nucleation.

An explanation for these apparently conflicting results can possibly be derived from the triglyceride composition of the HP. It consists of a fairly wide range of triglycerides, each having their own melting enthalpy and melting temperature. Triglycerides containing short fatty acids will have a lower melting enthalpy and melting temperature than those containing long-chain fatty acids. The solubility of triglycerides in oil depends on their melting enthalpy and melting temperature; it decreases with decreasing temperature. Whether a triglyceride or a group of triglycerides is supersaturated depends on both solubility and the amount of those triglycerides present. Triglycerides that contain long-chain fatty acids (C20, C22) are only present at very small fractions and would not be supersaturated at conditions at which bulk crystallization occurs: bulk crystallization will be initiated by heterogeneous nucleation of triglycerides containing shorter fatty acids (C16, C18). In the case of emulsified 10% HP/SF, crystallization occurs at much lower temperatures, at which (groups of) triglycerides containing long-chain fatty acids, present at small amounts, would be supersaturated. About 3% of the triglycerides in HP consist of fatty acid residues with

lengths of 18 and 20 carbon atoms. Suppose this group has a melting enthalpy and melting temperature in the  $\alpha$  polymorph of 125 kJ·mol<sup>-1</sup> and 62.9°C, respectively. These values are the average of the values for tristearate (C18) and tricosteanate (C20). The mole fraction soluble HP in SF ( $x_{\text{HP}}$ ) as a function of temperature can be calculated using the Hildebrand equation (Eq. 1), which assumes ideal mixing behavior (5,6). Dispersed 10% HP/SF with sodium caseinate as emulsifier started to crystallize at a temperature of about 10°C. At this temperature the solubility of triglycerides containing C18 and C20 fatty acids is about 0.02% in the  $\alpha$  polymorph. A 10% HP/SF mixture contains 10% · 3% = 0.3% of these triglycerides, i.e., considerable supersaturation. The supersaturation ( $\ln \beta$ ) of the triglycerides containing long-chain fatty acids is about 2.7, while the "overall" supersaturation calculated from the bulk properties is about 1.9. Whether using the bulk properties or those of triglycerides containing long-chain fatty acids, a supercooling of 14 K is calculated, although there is a considerable difference in supersaturation. This implies that the degree of supercooling would not be a good criterion to decide whether nucleation is homogeneous or heterogeneous. A better criterion may be the supersaturation, but this parameter is difficult to define in mixtures that contain a wide distribution of triglycerides.

Can we now explain why the crystallization kinetics of emulsified HP fits a heterogeneous nucleation model, whereas the supercooling or supersaturation needed to achieve crystallization is independent of average particle size? When fitting the crystallization curves of emulsified HP with a heterogeneous nucleation model, the nucleation rate is assumed to decrease with time. This is because the size of the droplets that crystallize decreases in time, and so does the number of impurities per droplet. However, if the catalytic impurities are formed by a group of triglycerides that is present in small amounts but are the most supersaturated, the number of triglyceride molecules per droplet and their molecular collision frequency can be the limiting factor for nucleation to occur. In that case nucleation would be catalyzed by groups of triglyceride molecules that are present in such small amounts, and the kinetics are modeled best by a heterogeneous nucleation mechanism; in reality the nucleation type is homogeneous, by being catalyzed by the triglycerides themselves. The reason that the crystallization temperature does not strongly decrease with decreasing particle size can be due to the narrow triglyceride composition. If the number of mol-

ecules of a certain group of triglycerides per droplet becomes too small for the occurrence of nucleation in smaller droplets, only a little further cooling is needed to increase the nucleation rate by the same factor as that by which the droplet volume is reduced, because the Gibbs activation energy for nucleation is strongly temperature dependent. Furthermore, the number of molecules ( $N$  in Eq. A-1) that can participate in forming a catalytic unit will increase with a small decrease in temperature. Performing calculations on the extent of supersaturation of certain groups of triglycerides at relevant temperatures would be very difficult, since accurate thermodynamic data are not available. Moreover, the formation of compound crystals will greatly complicate the theory.

From Figures 4 and 6 it is clear that, in agreement with classical nucleation theory, a linear relation exists between  $\ln J$  and the supersaturation term  $1/(T \cdot \Delta^2 T)$  for the sodium caseinate-stabilized emulsions. From the slope and the intercept, an (apparent) Gibbs surface energy of a nucleus and the pre-exponential frequency term may be calculated (Table 5). From the homogeneous nucleation rates of dispersions containing 10% HP/SF stabilized with sodium caseinate, a Gibbs surface energy of 4.1 mJ·m<sup>-2</sup> was calculated. If the same dispersed phase was stabilized with Tween 20, a Gibbs surface energy of 3.3 mJ·m<sup>-2</sup> was obtained. The difference would be caused by the heterogeneous nucleation mechanism instead of homogeneous nucleation. There was no big difference in the calculated  $\gamma$  (about 5%) if for the same sodium caseinate stabilized 10% HP/SF emulsion heterogeneous nucleation was assumed to occur instead of homogeneous nucleation.

The calculated Gibbs surface energies are much smaller than the values determined by Phipps (1), or Skoda and van den Tempel (2) for emulsified tristearate and tripalmitate. They found values of about 10 mJ·m<sup>-2</sup>. This may be due to purity of the crystallizing phase and therefore the availability of more accurate thermal data. Figure 9 compiles literature data of nucleation rates in various dispersed phases as a function of a supercooling term. The nucleation rate for the model system with paraffin oil as the liquid phase strongly deviates, which may be due to the nature of the liquid phase.

Pre-exponential frequency terms were about 10<sup>21</sup> m<sup>-3</sup>·s<sup>-1</sup> for homogeneous nucleation. If it is assumed that nucleation is homogeneous and we take the bulk properties of 10% HP/SF ( $N = 7 \cdot 10^{25}$  molecules·m<sup>-3</sup>,  $T = 288$  K, and  $\Delta S = \Delta H_{f,\alpha}/T_{m,\alpha} = 311$  J·mol<sup>-1</sup>(K<sup>-1</sup>), the fraction  $\alpha$  of the molecule that should be in the right conformation for incorporation in a

**TABLE 5**  
Apparent Gibbs Surface Energy ( $\gamma$ ) of a Nucleus and the Frequency Term Obtained from Isothermal Crystallization of Emulsified HP/SF Mixtures Nucleating in the  $\alpha$  Polymorph

HP/SF (%)	Emulsifier	Nucleation type (from fit)	$\gamma$ (mJ·m <sup>-2</sup> )	Pre-exponential factor (m <sup>-3</sup> ·s <sup>-1</sup> )	$r^2$
100	Caseinate	Heterogeneous	2.6	4.7 · 10 <sup>19</sup>	0.9995
10	Caseinate	Homogeneous	4.1	1.9 · 10 <sup>21</sup>	0.9927
10	Tween 20	Heterogeneous	3.3	8.6 · 10 <sup>19</sup>	0.9400

<sup>a</sup> $r$ , correlation coefficient. For other abbreviations see Table 1.



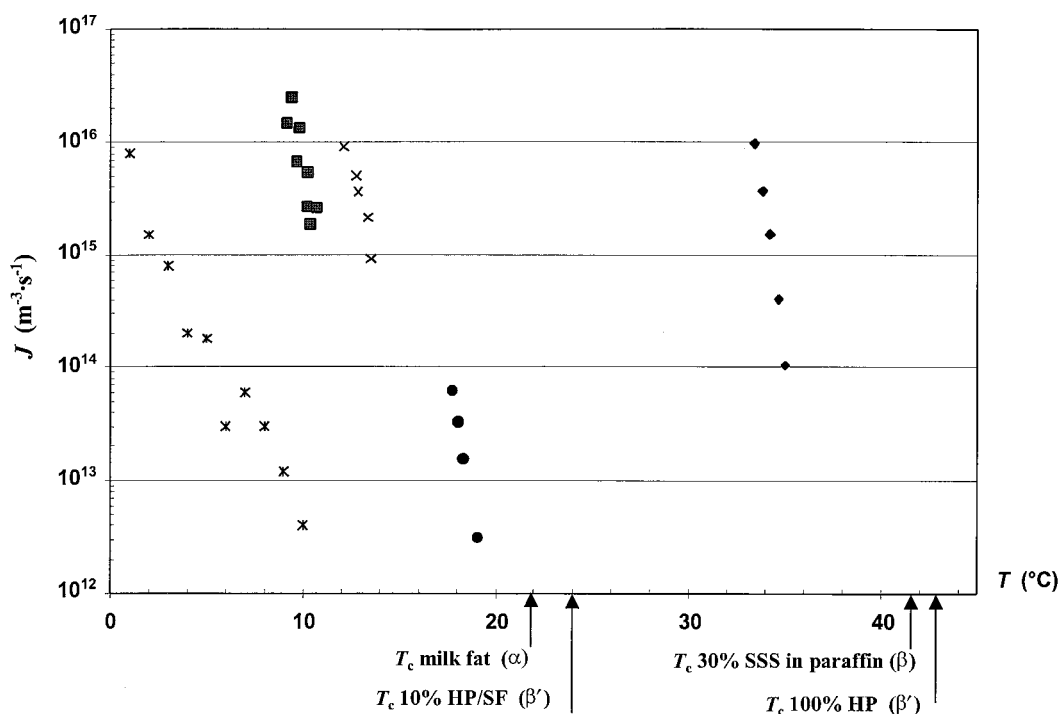


FIG. 9. Nucleation rates ( $J$ ) as a function of temperature ( $T$ ) in various systems.  $\blacklozenge$  100% HP;  $\blacksquare$  10% HP/SF in Na-caseinate;  $\times$  10% HP/SF in Tween 20;  $\times$  tristearin (TSS)/milk fat (3);  $\bullet$  30% SSS in paraffin (2). Clear points ( $T_c$ ) are indicated. See Figure 2 for abbreviations.

nucleus according to Equation A-1 is 1.08. If it is assumed that only triglycerides having C18 and C20 fatty acids (3% of the HP) can form nuclei, values for  $\Delta H_{f,\alpha} = 125 \text{ kJ}\cdot\text{mol}^{-1}$  and  $T_{m,\alpha} = 336 \text{ K}$ , lead to  $\alpha \approx 0.98$ . These values indicate that virtually the whole triglyceride molecule should be in the right conformation for incorporation in a nucleus. This seems very unlikely. It is expected that a smaller proportion of the triglyceride molecule should be in the right conformation: the rest of the triglyceride molecule can be incorporated relatively easily in a nucleus. The high value of  $\alpha$  suggest that there are other factors that delay the formation of a nucleus.

APPENDIX

The number of nuclei that are formed per unit volume and unit time is called the nucleation rate  $J$  and is mostly expressed as an Arrhenius-type of equation (15) although it may be criticized (16).

$$J = N \cdot \frac{k_b T}{h} \cdot \exp\left(\frac{-\alpha \cdot \Delta S}{R_g}\right) \cdot \exp\left(\frac{-\Delta G_{3D}^*}{k_b T}\right) \quad [A-1]$$

The term  $N \cdot (k_b T/h)$  is the maximum collision frequency in a system containing  $N$  molecules,  $k_b$  the Boltzmann constant,  $T$  the temperature, and  $h$  the Planck constant. The second term incorporates the fact that a molecule has to be in the right conformation (or nearly so) before it can be incorporated in a nucleus. This term will be important for long-chain molecules and depends on the molar loss of entropy  $\Delta S$  on incorporation in a nucleus, which is given by  $\Delta H_{f,i}/T_{m,i}$ ; the fraction  $\alpha$  of

the molecule that should be in the right conformation; and  $R_g$ , the gas constant. The molar loss of entropy  $\Delta S$  on incorporation in a nucleus is given by  $\Delta H_{f,i}/T_{m,i}$  where  $\Delta H_{f,i}$  is the molar enthalpy of fusion and  $T_{m,i}$  the absolute melting temperature in polymorph  $i$ . The third term is due to the Gibbs activation energy  $\Delta G_{3D}^*$  for formation of a nucleus with critical size. The latter is given by:

$$\Delta G_{3D,hom}^* = \frac{16\pi \cdot v_c^2 \cdot \gamma^3 \cdot N_{av}^2}{3 \cdot \Delta\mu^2} \quad [A-2]$$

$$\Delta\mu_{\text{solution}} = R_g T \cdot \ln\beta \quad \Delta\mu_{\text{melt}} = \Delta H_{f,i} \cdot \frac{T_{m,i} - T}{T_{m,i}}$$

where  $\beta$  is the supersaturation ratio which gives the ratio between the solubilities of the crystallizing component at saturated and supersaturated conditions,  $v_c$  the molecular volume in a crystal,  $N_{av}$  Avogadro's number,  $\Delta\mu$  the difference in chemical potential, and  $\gamma$  the Gibbs surface energy.

Nucleation rates in emulsified fats can be determined by measuring the volume fraction of solid fat ( $\phi$ ) as a function of time ( $t$ ). One must assume that the average time needed for a nucleation event is much longer than the time needed for the droplet to achieve complete crystallization. In that case, the volume crystallization rate is determined by the nucleation rate (17–19). By taking into account the droplet size distribution of the emulsion, the fraction of crystallized droplets is given by:

$$\phi = 1 - \int_0^\infty \phi_d^0 \cdot \exp(-k \cdot t) dd \quad [A-3]$$

where  $\phi_d^0$  is the differential volume fraction of droplets with sizes between  $d$  and  $d + dd$ . Neglecting the droplet size distribution by using only the average droplet diameter may greatly affect the results. Furthermore,  $k$  is a rate constant, which is given by  $J \cdot v_d$  where  $v_d$  is the droplet volume or by  $J \cdot a_d$  where  $a_d$  is the droplet surface area. In the case of homogeneous volume nucleation or nucleation catalyzed by the homogeneous droplet boundary, the isothermal crystallization rate can be modeled by only one nucleation rate independent of  $d$ . It is assumed that the droplet composition and the composition of the droplet surface are invariant of  $d$ .

In case of heterogeneous nucleation, the crystallization volume contains impurities that catalyze the nucleation process. This nucleation process cannot be modeled by a single nucleation rate, because the number of impurities per droplet varies with diameter or surface area. Furthermore, there is a distribution in the catalytic activity of the impurities. The nucleation rate decreases with time. At the start of the heterogeneous nucleation process, the droplets containing the highest number of catalytic impurities will crystallize. This maximum nucleation rate  $J_0$  may roughly be related to the nucleation rates in bulk fats. As crystallization proceeds, smaller droplets will crystallize because they contain fewer impurities. At the end of the crystallization process, the volume fraction of solidified droplets will reach a plateau value  $\phi_m$  because some droplets are void of impurities and therefore will not nucleate heterogeneously. If it is assumed that the catalytic impurities are distributed at random over the volume, the maximum achievable volume fraction of solid droplets can be related to the number of impurities per volume by:

$$\phi_m = 1 - \exp(-v_d \cdot N_{\text{imp}}) \quad [\text{A-4}]$$

where  $N_{\text{imp}}$  is the number density of catalytic impurities, which is strongly dependent on temperature. Walstra and van Beresteyn (3) showed that the nucleation rate could approximately be written as function of the initial, i.e., maximum nucleation rate  $J_0$  and the volume fraction of solid droplets by the following relation:

$$\phi = \frac{-1 + \exp\left[J_0 \cdot v_d \cdot t \cdot (\phi_m - 1) / \phi_m\right]}{-(1/\phi_m) + \exp\left[J_0 \cdot v_d \cdot t \cdot (\phi_m - 1) / \phi_m\right]} \quad [\text{A-5}]$$

Fitting crystallization curves of emulsified triglycerides to a heterogeneous nucleation model (Eqs. A-4 and A-5) requires the fit parameters  $J_0$  and  $N_{\text{imp}}$  whereas a homogeneous nucleation model (Eq. A-3) requires only one nucleation rate as a fit parameter.

## ACKNOWLEDGMENTS

This research was funded by the research organization Renolvet and the TNO Institute for Food and Nutrition. We thank Dr. M.J.W. Povey from the Procter Department of Food Science of Leeds Uni-

versity for his hospitality and help with ultrasound velocity measurements. Martine van den Berg is thanked for her contribution to the DSC and p-NMR experiments.

## REFERENCES

1. Phipps, L.W., Heterogenous and Homogeneous Nucleation in Supercooled Triglycerides and *n*-Paraffins, *Trans Faraday Soc.* 60:1873–1883 (1964).
2. Skoda, W., and M. van den Tempel, Crystallization of Emulsified Triglycerides, *J. Colloid Sci.* 18:568–584 (1963).
3. Walstra, P., and E.C.H. van Beresteyn, Crystallization of Milk Fat in the Emulsified State, *Neth. Milk Dairy J.* 29:35–65 (1975).
4. Walstra, P., T. van Vliet, and W. Kloek, Crystallization and Rheological Properties of Milk Fat, in *Advanced Dairy Chemistry Vol. 2; Lipids*, 2nd edn., edited by P.F. Fox, Chapman & Hall, London, 1995, pp. 179–211.
5. Wesdorp, L.H., *Liquid-Multiple Solid Phase Equilibria in Fat—Theory and Experiments*, Ph.D. Thesis, Technical University of Delft, Delft, The Netherlands, 1990, 258 pp.
6. Hannewijk, J., Kristallisatie Van Vetten I, *Chem. Weekbl.* 60:309–316 (in Dutch) (1964).
7. Kloek, W., P. Walstra, and T. van Vliet, Crystallization Kinetics of Fully Hydrogenated Palm Oil in Sunflower Oil Mixtures, *J. Am. Oil Chem. Soc.* 77:389–398 (2000).
8. van Boekel, M.A.J.S., *Influence of Fat Crystals in the Oil Phase on Stability of Oil-in-Water Emulsions*, Ph.D. Thesis Wageningen Agricultural University, Wageningen, The Netherlands, 1980, 98 pp.
9. van Putte, K., and J.C. van den Enden, Fully Automated Determination of the Solid Fat Content by Pulsed NMR, *J. Am. Oil Chem. Soc.* 51:316–320 (1974).
10. Povey, M.J.W., Ultrasound Studies of Shelf-Life and Crystallization, in *New Physico-Chemical Techniques for the Characterization of Complex Food Systems*, edited by E. Dickinson, Chapman & Hall, London, 1995, pp. 196–212.
11. Povey, M.J.W., *Ultrasonic Techniques for Fluids Characterization*, Academic Press, San Diego, 1997, pp. 54–76.
12. Dickinson, E., D.J. McClements, and M.J.W. Povey, Ultrasonic Investigation of the Particle Size Dependence of Crystallisation in *n*-Hexadecane–Water Emulsions, *J. Colloid Interface Sci.* 142:103–110 (1991).
13. Hodate, Y., S. Ueno, J. Yano, T. Katsuragi, Y. Tezuka, T. Tagawa, N. Yoshimoto, and K. Sato, Ultrasonic Velocity Measurement of Crystallization Rates of Palm Oil in Oil–Water Emulsions, *Colloids Surf. A128*:217–224 (1997).
14. Kaneko, N., T. Horie, S. Ueno, J. Yano, T. Katsuragi, and K. Sato, Impurity Effects on Crystallization Rates of *n*-Hexadecane in Oil-in-Water Emulsions, *J. Crystal Growth* 197:263–270 (1999).
15. Volmer, M., *Kinetik der Phasenbildung*, Steinkopff, Leipzig, 1939, 134 pp.
16. Lyklema, J., *Fundamentals of Interface and Colloid Science, Vol. I, Fundamentals*, Academic Press, London, 1991, 205 pp.
17. Turnbull, D., Kinetics of Solidification of Supercooled Liquid Mercury Droplets, *J. Chem. Phys.* 20:411–424 (1952).
18. Turnbull, D., and J.C. Fisher, Rate of Nucleation in Condensed Systems, *Ibid.* 17:71–73 (1949).
19. Turnbull, D., and R.L. Cormia, Kinetics of Crystal Nucleation in Some Normal Alkane Liquids, *Ibid.* 34:820–831 (1960).
20. Kashchiev, D., N. Kaneko, and K. Sato, Kinetics of Crystallization in Polydisperse Emulsions, *J. Colloid Interface Sci.* 208:167–177 (1998).

[Received April 29, 1999; accepted March 8, 2000]